

# Optoelectronic Microwave-Range Frequency Mixing in Semiconductor Lasers

Efim L. Portnoi, *Member, IEEE*, Vera B. Gorfinkel, Eugene A. Avrutin, Iain G. Thayne, David A. Barrow, John H. Marsh, *Senior Member, IEEE*, and Serge Luryi, *Fellow, IEEE*

**Abstract**— Optoelectronic mixing of very high-frequency amplitude-modulated signals using a semiconductor laser simultaneously as a local oscillator and a mixer is proposed. Three possible constructions of a monolithically integrated up- or down-converter are considered theoretically: a four-terminal semiconductor laser with dual pumping current/modal gain control, and both a passively mode-locked and a passively  $Q$ -switched semiconductor laser monolithically integrated with an electroabsorption or pumping current modulator. Experimental verification of the feasibility of the laser-mixer concept is presented.

## I. INTRODUCTION

**F**REQUENCY mixing, along with signal generation and amplification, is one of the basic functions of electronics. However, in present-day optoelectronic systems, using amplitude-modulated optical signals, this function is not yet properly realized. All the optoelectronic mixers proposed to date produce an *electrical* intermediate-frequency (IF) output [1], whereas the ease with which high-frequencies can be handled optoelectronically suggests that a mixing element should be developed which provides its output in the form of an amplitude-modulated *optical* signal. In this paper, we propose the use of a semiconductor laser to perform such an optical mixing operation. We shall concentrate on technologically simple monolithically integrated versions of the laser-mixer, three of which are shown schematically in Fig. 1. Fig. 1(a) shows the mixer in the form of a four-terminal laser with dual (current and confinement) modulation [2], [3]. Alternatively, the laser could contain a saturable absorber within the cavity [4]–[9] to achieve either high frequency  $Q$ -switching (Fig. 1(b)) or mode-locking (Fig. 1(c)) to provide oscillations of the photon and electron densities at a local oscillator frequency  $f_{LO}$ . Oscillation of the modal gain at

Manuscript received November 3, 1994; revised February 7, 1995. This work was supported in part by the Engineering and Physical Sciences Research Council (Grant Number GR/H/82471). One of the authors (E. L. Portnoi) was supported in part by the University of Glasgow. One of the authors (I. G. Thayne) was supported in part by an EPSRC Postdoctoral Research Fellowship. One of the authors (D. A. Barrow) was supported in part by a CASE award with BNR (Europe).

E. L. Portnoi is with the A. F. Ioffe Physico-Technical Institute, St. Petersburg 1941024 Russia.

V. B. Gorfinkel is with the Dept. of High Frequency Engineering, University of Kassel, Kassel D-34121, Germany.

E. A. Avrutin, I. G. Thayne, D. A. Barrow, and J. H. Marsh are with the Dept. of Electronics & Electrical Engineering, University of Glasgow, Glasgow G12 8QQ Scotland, UK.

S. Luryi is with the Dept. of Electronics & Electrical Engineering, State University of New York, Stony Brook, NY 11794-2350 USA.

IEEE Log Number 9411389.

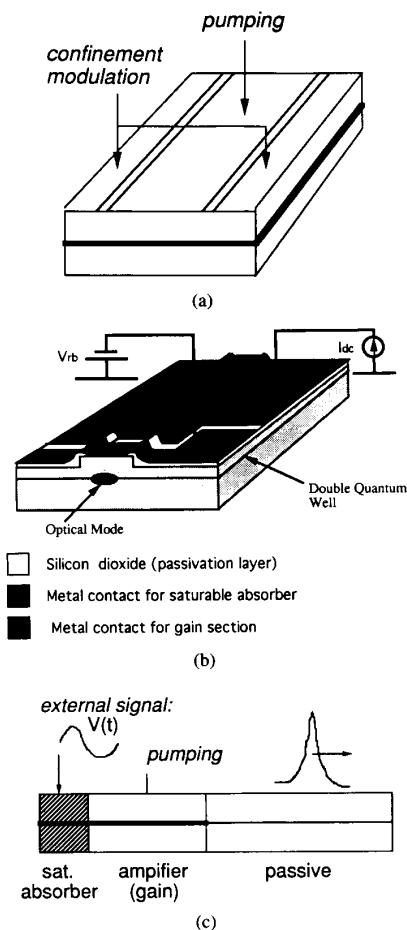


Fig. 1. Schematic of integrated laser-mixer constructions: (a) Four-terminal laser with dual current/confinement modulation. (b) Double-section laser with current modulation (the actual structure used in our experiments). (c) Monolithic extended-cavity laser with electroabsorption-modulated saturable absorber.

the signal frequency  $f_S$  may be achieved in the latter two cases by modulation of either the pumping current (for the  $Q$ -switching range of frequencies) or the carrier confinement or photon lifetime (at higher mode-locking frequencies). Mixing of the local oscillator and the signal in all three cases occurs due to parametric effects since the induced recombination rate depends on the product of the modal gain and photon density.

The mixing schemes we propose are attractive for very high frequencies. Indeed, it has been shown theoretically that efficient very high-frequency modal gain modulation can be achieved in a 4-terminal semiconductor laser structure [2], [3]. Passive mode-locking can generate picosecond optical pulses at even higher repetition rates, moving from hundreds of GHz [4] to the terahertz range as new techniques [5], [6] are introduced, the average powers available being up to hundreds of mW [7].

This paper consists of two main sections, in which frequency mixing in semiconductor lasers is studied theoretically (Section II) and experimentally (Section III).

## II. THEORY

### A. Laser with Dual Modulation

Here, we utilize the usual method for treating frequency mixing and conversion, which is to assume that the system (the laser) is subject to external modulation at two different RF frequencies, the local oscillator frequency  $f_{LO}$ , and the signal frequency  $f_S$ . For simplicity it is assumed throughout the paper that the frequencies are not integer multiples of each other. Assuming the frequencies are not ultrahigh (i.e., they are lower than the laser cavity round trip frequency), we can describe the laser by the standard system of rate equations

$$\frac{dN}{dt} = J - \frac{N}{\tau_N(N)} - \nu_g g(N)S \quad (1a)$$

$$\frac{dS}{dt} = \left( \Gamma g(N) - \frac{1}{\tau_{ph}} \right) S + R_{sp} \quad (1b)$$

where the notations are mostly standard and self-explanatory and are defined in Table I. We assume that the laser is operating well above threshold so that lasing is well-developed, and the last (spontaneous) term in (1b) can therefore be neglected in this section.

Following [2], [3], we assume that, along with conventional RF modulation of the pumping current  $J$  we can also impose some (small) modulation in the confinement factor  $\Gamma$ , at a different RF frequency. Either of these methods of modulation can be used to provide the local oscillator and/or the signal. One can then distribute the "dynamical variables" of the system (i.e., carrier and photon densities) into frequency components in the following way:

$$\begin{aligned} N &= N_0 + N_{LO} \exp(i\omega_{LO}t) + N_s \exp(i\omega_S t) \\ &\quad + \sum_{\omega_2} N_{\omega_2} \exp(i\omega_2 t) + \text{c.c.} \\ S &= S_0 + S_{LO} \exp(i\omega_{LO}t) + S_s \exp(i\omega_S t) \\ &\quad + \sum_{\omega_2} S_{\omega_2} \exp(i\omega_2 t) + \text{c.c.} \end{aligned} \quad (2)$$

where the "second-order" frequencies  $\omega_2 = \omega_{LO} \pm \omega_S$ ,  $2\omega_{LO}$ ,  $2\omega_S$  arise from beating between the "first-order" frequencies. Note that these formulae are independent of which of the two modulation methods provides the signal and which one acts as the local oscillator.

Substituting (2) into the system (1), linearising and writing out equations for the amplitudes of each harmonic separately

TABLE I  
LASER DIODE PARAMETERS USED IN COMPUTATIONS

Parameter	Symbol	Value in	Value in	Unit
		Subsection 2.2	Subsection 2.3	
gain (in gain section)	$g$	$\nu_g A_g (N - N_{0g}) (1 - \epsilon_g S)$		1/s
absorption (in saturable absorber section)	$a$	$\nu_g A_a (N_{0a} - N) (1 - \epsilon_a S)$		1/s
electron lifetime (in gain section)	$\tau_N$	$1/BN$		s
photon lifetime	$\tau_{ph}$	$2L/(\nu_g \ln(1/R))$		s
pumping current in gain section	$J_g$			
pumping current in saturable absorber section	$J_a$	0		
active layer thickness	$d$			
bimolecular recombination coefficient	$B$	$1.5 \cdot 10^{10}$		cm <sup>3</sup> /s
spontaneous emission factor	$\beta_{sp}$	$10^{-4}$		
recombination time in saturable absorber section	$\tau_a$	0.01		ns
group velocity of light	$\nu_g$	$0.75 \cdot 10^{10}$		cm/s
confinement factor	$\Gamma$	0.08	0.05	
saturable absorber (SA) length fraction	$r_a$	0.088	0.037	
gain length fraction	$r_g$	$1 - r_a$	0.336	
gain cross section	$A_g$	$4 \cdot 10^{-16}$		cm <sup>2</sup>
SA cross section	$A_a$	$10 \cdot 10^{-16}$	$16 \cdot 10^{-16}$	cm <sup>2</sup>
effective transparency carrier density, gain section	$N_{0g}$	$1.2 \cdot 10^{18}$		cm <sup>3</sup>
effective transparency carrier density, SA section	$N_{0a}$	$2.6 \cdot 10^{18}$	$1.2 \cdot 10^{18}$	cm <sup>3</sup>
gain suppression coefficient	$\epsilon_g$	$5 \cdot 10^{-18}$		cm <sup>3</sup>
saturable absorber suppression coefficient	$\epsilon_a$	$5 \cdot 10^{-18}$		cm <sup>3</sup>
intensity reflection coefficients (both sides)	$R$	0.36		
linewidth enhancement factor	$\alpha$		2	
gain linewidth	$\Delta\Omega_g$		$2 \cdot 10^{13}$	1/s
laser cavity length	$L$	400	1875	$\mu\text{m}$

(harmonic balance method), expressions for the amplitudes of the optical signal at the "second-order" frequencies may be derived:

$$\begin{aligned} S_{\omega_2 = \omega_i \pm \omega_k} &= \Delta\Gamma \left[ 1 + \frac{1}{S_0 g'_N} \left( i\omega_2 + \frac{1}{\tau_{Nd}} \right) \right] \\ &\quad + \left( i\omega_2 + \frac{1}{\tau_{Nd}} \right) \frac{1}{S_0} S \otimes N \left/ \left( i\omega_2 + \frac{1}{\tau_{Nd}} \right) \frac{i\omega_2}{\Gamma_0 S_0 g'_N} \right. \\ &\quad \left. + \left( g_0 + \frac{i\omega}{\Gamma_0} \right) \right] \quad (3a) \end{aligned}$$

where the additional notations

$$\Delta\Gamma = \frac{g'_N S_0}{\Gamma_0} \Gamma \otimes N + \frac{g_0}{\Gamma_0} \Gamma \otimes S \quad (3b)$$

$$\begin{aligned} 1/\tau_{Nd} &= 1/N \cdot \partial/\partial N (N/\tau_N); \\ g'_N &= \partial g/\partial N; \quad g_0 = g(N_0) \end{aligned} \quad (3c)$$

$$\begin{aligned} (X \otimes Y)_{\omega_i - \omega_k} &= X_{\omega_i} Y_{\omega_k}^* + Y_{\omega_i} X_{\omega_k}^*; \\ (X \otimes Y)_{\omega_i \omega_k} &= X_{\omega_i} Y_{\omega_k} + Y_{\omega_i} X_{\omega_k} \end{aligned} \quad (3d)$$

have been introduced.

As can be seen from (3), the value of  $S_{\omega_2}$  for the case of beat frequency is directly proportional to the amplitudes  $S$ ,  $N$  and  $\Gamma$  at the first-order frequencies  $f_S = \omega_S/2\pi$  and  $f_{LO} = \omega_{LO}/2\pi$ . The denominator in (3a) is essentially the same resonant denominator one finds in the usual formulae for

the modulation response of a laser diode. For the important case of down-conversion with small difference frequencies  $f_2 \ll f_{\text{res}}$ , ( $f_2 = \omega_2/2\pi$ , and  $f_{\text{res}} = 1/2\pi \cdot \sqrt{S_0 \cdot g'_N/\tau_{ph}}$  is the electron-photon resonance frequency), this denominator depends weakly on  $f_2$ . Therefore, for an external RF signal, provided that  $f_{LO} \gg f_{\text{res}}$  and  $f_{LO} \sim f_S$ , the frequency dependence of the down-conversion efficiency will be determined by the amplitudes of  $S_{LO}$ ,  $N_{LO}$ ,  $S_s$ , and  $N_s$ . The frequency dependence of these parameters clearly depends on the mechanisms of the corresponding modulation method. A simple analysis shows that, in the case when both the LO and the signal are provided by current modulation, the amplitude of the intermediate-frequency signal decays at high signal frequencies as  $1/f_{LO}^3$  which makes the use of such modulation very inefficient at high frequencies. However, if at least one of the modulating frequencies (local oscillator and/or signal) were due to confinement variation, both response amplitudes would decay at high frequencies only as  $1/f$ . Therefore, in a laser with dual modulation, confinement variation should be efficient as the modulation scheme for both the local oscillator and the signal. It can be easily shown that the same argument holds if, instead of modulating  $\Gamma$ , one is able to modulate any other variable which affects the net mode gain directly (rather than indirectly, as does pumping modulation). For instance, fast modulation of the cavity loss would be a suitable technique [8].

Another way of achieving efficient modulation of laser light at the RF frequency  $f_{LO}$  is to utilize some regime whereby such oscillations are generated within the laser itself, rather than resulting from external modulation. This can be achieved by introducing a saturable absorber section into the laser cavity, which results either in repetitive  $Q$ -switching (self-pulsations), or in passive mode-locking.

### B. Laser with Saturable Absorber: Passive $Q$ -Switching

To describe a passively  $Q$ -switched laser, the system (1) is completed by an equation describing the carriers in the (fast) saturable absorber; the equation for light is modified accordingly to obtain [9]:

$$\frac{dN_g}{dt} = J_g - \frac{N_g}{\tau_N(N_g)} - gS_g \quad (4a)$$

$$\frac{dN_a}{dt} = J_a - \frac{N_a}{\tau_a} + aS_a \quad (4b)$$

$$\frac{dS}{dt} = \left[ \Gamma(r_g g - r_a a) - \frac{1}{\tau_{ph}} \right] \cdot S + \beta_{sp} \frac{N_g}{\tau_N(N_g)} \quad (4c)$$

where  $N_g$  and  $N_a$  are the carrier densities in the gain and absorber sections of the laser cavity, respectively;  $r_g$  and  $r_a$  denote the volume fractions occupied by corresponding sections;  $a$  is the saturable absorption coefficient in the corresponding section.  $S_g$  and  $S_a$  are the photon densities averaged through these respective sections (to a first approximation,  $S_a = S_g = S$ , although this assumption is not made in our model which uses simple formulae for  $S_g$  and  $S_a$  derived in [9]).

The approach of the previous section can be applied to (4) resulting in a formula qualitatively similar to (3), in which

$N_{LO}$  and  $S_{LO}$  are now due to self-pulsations, the frequency  $f_{LO}$  being the self-pulsing frequency. However, the light modulation under self-pulsing is well known to be highly nonsinusoidal; therefore the predictions of the small-signal formula (3) are essentially only qualitative, which makes the use of a more complete, numerical, calculation necessary. The numerical calculations are performed here for a tandem laser structure consisting of adjacent gain and absorber sections within a common cavity, the same laser configuration studied in [9]. The parameter values used in the model are listed in Table I and chosen so as to correspond approximately to the experimental situation described hereafter (Section III); namely, the geometry of the laser was chosen close to that studied in the experiments and the parameters of the saturable absorber fitted to provide a) similar increase in threshold due to implementation of the  $SA(J_{th}/J_{th(0)} = 1.8)$  and b) similar  $Q$ -switching frequency at given current level ( $f_{LO} = 1.5$  GHz at  $J/J_{th(0)} = 4$ ). The signal is applied in the form of a sinusoidal modulation of the pumping current in the gain section:  $J_g = J_{g0} + \Delta J_g \sin(2\pi f_S t)$ .

We now study the behavior of the laser under external modulation at a constant frequency  $f_S$  and increasing amplitude  $\Delta J_g$ . Fig. 2 shows examples of the calculated time-dependent profiles of the  $Q$ -switched pulses without (Fig. 2(a)) and with (Fig. 2(b)) external modulation. The modulation imposes a slow envelope on the pulse train which is, in general, of a nonsinusoidal form. To understand the effect of the modulation more quantitatively, we perform Fourier transforms of the observed light signals, so obtaining the RF spectra. The low-frequency parts of these spectra are illustrated in Fig. 3, where (a) and (b) correspond to Fig. 2(a) and 2(b), respectively. Fig. 3(a), with  $\Delta J_g = 0$ , shows the spectrum of clear self-pulsation, which, as expected, consists of a set of narrow lines (of which only the first two are shown) at the frequency  $f_{LO}$  and its integer harmonics. As one applies a weak RF modulation at  $f_S$  (Fig. 3(b)), spectral lines appear at the difference beat frequency  $|f_S - f_{LO}|$  and at the sum beat frequency  $f_S + f_{LO}$  thus showing that both down- and up-conversion are taking place. Another line can be seen at  $2f_{LO} - f_S$ , which, at least for low modulation amplitudes, may be regarded as the result of the mixing between the signal at  $f_S$  and the second harmonic of  $f_{LO}$ . As the modulation amplitude is increased, the intensities of the beat frequency lines increase as well. We use these intensities to evaluate the efficiency of up- and down conversion, defined as

$$\eta = \Theta \frac{P_2}{P_s} \quad (5)$$

where the factor  $\Theta \approx (1-R)/2$ ,  $R$  being the facet reflectivity, approximately relates the average intensity in the laser, used in (4), to the intensity emitted through one of the two facets.  $P_2$  is the power at the difference frequency  $f_2 = f_{LO} \pm f_S$  calculated from the RF spectra of the variable  $S$  computed through (4), and  $P_s$  is the input signal power estimated as  $P_s = \hbar\omega \cdot \Delta I_g \cdot V$ ,  $V$  being the active layer volume. Fig. 3(c) (solid lines) shows these efficiencies versus the amplitude of the modulation current, measured as a fraction of the threshold current  $J_{th(0)}$  of a fully forward biased

laser. One sees that the efficiencies, particularly that of up-conversion, are of respectable order of magnitude even for the modest LO intensities studied. Increasing the modulation amplitude, as is seen in Fig. 3(c), results in some saturation in conversion efficiency. It also leads to the emergence of a whole set of sidebands around  $f_{LO}$  and its harmonics, and also to the generation of a set of additional lines, arising from mixing between different first- and second-order frequencies, the latter signals being no longer negligible in amplitude. Some such lines, for example at  $2f_S - f_{LO} \sim 0.3$  GHz and at  $2f_S = 1.8$  GHz, are already present, with a small amplitude, in Fig. 3(b), and at  $\Delta J_g/J_{th(0)} \approx 0.4-0.5$ , the spectra become highly complex. The increase in modulation is also accompanied by a gradual pulling of the LO frequency toward that of the signal (by approximately 100 MHz within the limits of Fig. 3(c)), and if the modulation amplitude were to be increased further, above a certain threshold value ( $\Delta J_g/J_{th(0)} \approx 1.4$  in our case), abrupt frequency locking will occur and the spectrum will once more be a set of narrow lines, but now at harmonics of the signal frequency  $f_S$ . Such features, i.e., the generation of various combination frequencies (which is in fact a manifestation of the onset of increasingly complicated nonlinear dynamics, which may lead finally to optical chaos [10]), as well as frequency pulling, are clearly undesirable and will impose some limitations on the practical use of  $Q$ -switched lasers for optoelectronic frequency mixing. Other important limitations arise from the fact that the upper frequency limit of  $Q$ -switching, even with all the latest improvements in  $Q$ -switching schemes [11], does not exceed several tens of GHz, and from the vulnerability of the regime to noise-induced jitter [9]. Passive mode-locking, for which firmly stabilized repetition frequency is an essential feature, may be expected to be more free of such limitations. Therefore, having established in previous subsections the general principle of frequency mixing in laser diodes due to parametric effects, we now proceed to studying this last regime, which we consider to be the most important for very high frequency applications.

### C. Laser with Saturable Absorber: Passive Mode-Locking

1) *Model:* For a description of passive mode-locking, the single-mode lumped system (4) is clearly inadequate. We therefore use a model, similar in its main features to those of [12] and [13], in which the light propagation in the cavity is described by a propagation equation of the form

$$\begin{aligned} & \pm \frac{1}{v_g} \frac{\partial E_{R,L}}{\partial z} + \frac{\partial E_{R,L}}{\partial t} \\ & = \Gamma(\hat{g}E_{R,L} + i\alpha g E_{R,L}) + F_{rand} \end{aligned} \quad (6)$$

where  $E_{R,L}$  are properly normalized complex amplitudes of the field of the light wave propagating to the right and to the left respectively, and the operator  $\hat{g}$  includes a digital filter simulating gain dispersion [13]:

$$\hat{g}E = g \cdot \Delta\Omega_g \cdot \int_0^\infty E(t-\tau) \exp(-\Delta\Omega_g \cdot \tau) d\tau$$

where  $\Delta\Omega_g$  is the gain linewidth and  $g$  is the usual gain value used in the previous subsection. The last term in (6) represents

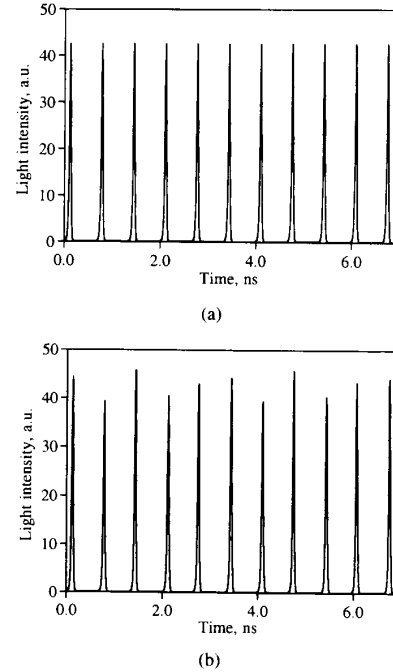


Fig. 2. (a) Fragment of a pulse train emitted by a free-running  $Q$ -switched laser diode; parameters as in Table I, pumping current  $J/J_{th(0)} = 4$  (self-pulsing frequency  $f_{LO} = 1.5$  GHz). (b) Same as in Fig. 2(a), under current modulation of an amplitude  $\Delta J_g/J_{th(0)} = 0.1$  applied to gain section.

a random noise source [13] and is essential for running the model. A self-induced grating (self-colliding-pulse effect) was also included in the calculations but did not affect the results significantly for our (uncoated-facet) structure. The dynamics of the carrier density are described by equations which are similar to 1(a) and 4(a) but are treated as local equations with

$$\begin{aligned} S &= |E_R|^2 + |E_L|^2 : \\ \frac{\partial N(z,t)}{\partial t} &= \frac{J(z,t)}{ed} - \frac{N}{\tau_N(z)} \\ &\quad - g(N)(|E_R(z,t)|^2 + |E_L(z,t)|^2). \end{aligned} \quad (7)$$

Within the saturable absorber sections the same equation holds, except that  $g$  becomes  $-a$  and the recombination time  $\tau(z)$  is adjusted accordingly (see Table I). Although the mode-locking regime is inherently capable of operating up to hundreds of GHz, in the bulk of this subsection we concentrate on the monolithic extended cavity laser construction, which includes a passive section in tandem with the gain and saturable absorber (SA) sections. The device is therefore designed to emit a pulse train at a moderate repetition frequency (20 GHz in our case), mainly to simulate realistically the parameters of the construction we plan to use in future experimental studies. Such lasers are usually made of QW material, and the passive waveguide can be fabricated for example using QW intermixing techniques [14]. The parameters are therefore chosen to correspond to a QW device and the signal is introduced as a direct modulation of the unsaturated absorption in the SA. In the experiment such modulation will be realized by modulating the reverse bias voltage applied to the SA section of the QW.

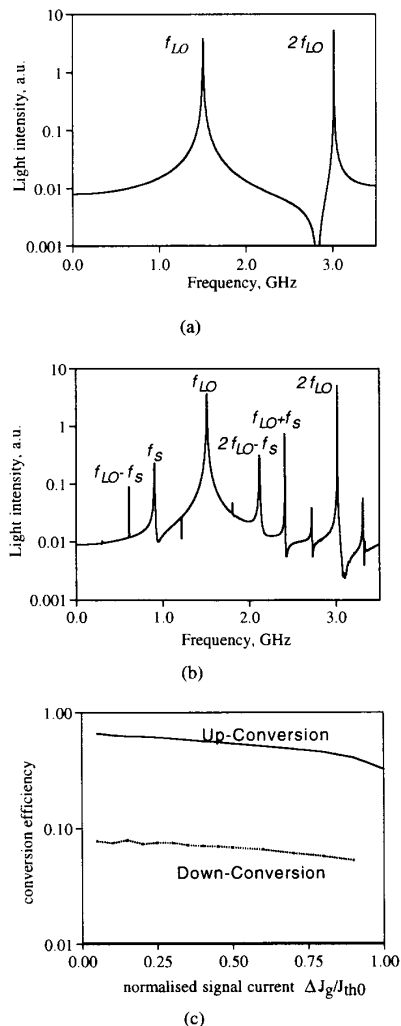


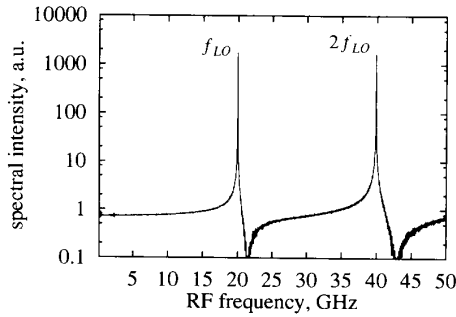
Fig. 3. (a) Part of the RF spectrum of a free-running  $Q$ -switched laser diode; parameters as in Table I, pumping current  $J/J_{th(0)} = 4$  (spectrum of signal shown in Fig. 2(a)). (b) The low-frequency part of the spectrum of the same laser, under current modulation at  $f_S = 0.9$  GHz with an amplitude  $\Delta J_g/J_{th(0)} = 0.1$  applied to gain section (spectrum of the signal shown in Fig. 2(b)). (c) Calculated efficiencies of up- and down-conversion versus modulation current. Parameters of the laser and pumping regime as in Figs. 2 and 3(a), (b).

This modulation technique is essentially a modulation in the photon lifetime, so, like confinement modulation discussed in Section II-A, it should [8] be more advantageous in the frequency range  $f_S \gg f_{res}$  than modulation of the pumping current.

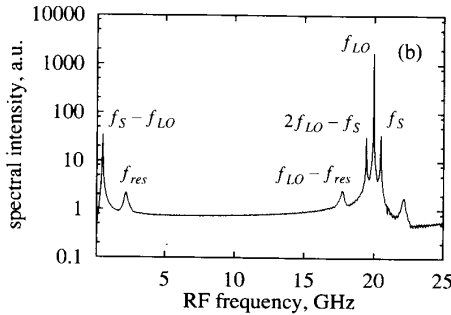
2) *Down-Conversion*: Fig. 4 shows the effect of external modulation on mode-locking spectra for the case of down-conversion. The qualitative similarity with the results obtained for  $Q$ -switching is clear, emphasizing the point made in Section II-B that, whichever effect is used to provide the LO, the fundamental physics of frequency mixing is essentially the same. However, there are some differences between the two regimes as well. In particular, since mode-locking is a much more “stiff” regime than  $Q$ -switching and the repetition

frequency is firmly fixed by the optical length of the cavity, the ranges over which frequency locking by external signal can occur are extremely narrow [15], [16]. Therefore, frequency mixing is possible for quite small frequency detuning (of the order of 0.1% of the repetition frequency) without the risk of pulling [15], [16]. Also, besides showing well-developed peaks at difference frequency and its harmonics, the spectra also contain additional small noise-like peaks, which may be associated with relaxation oscillations in the system at the frequency  $f_{res}$  (all calculated spectra exhibit also some general baseline intensity but this is due to numerical limitations; its level decreases with increased simulation time). One therefore expects that the conversion efficiency will be maximized if the local oscillator and signal frequency are resonantly adjusted so that  $f_S - f_{LO} = f_{res}$ . This is indeed confirmed by comparing Fig. 4(b) and (c); in the latter figure, this resonance condition is fulfilled approximately and the conversion efficiency is more than an order of magnitude higher than in the nonresonant case. However, as in the case of  $Q$ -switching, efficient conversion is accompanied by generation of multiple harmonics of the intermediate frequency, which is clearly undesirable in many applications. Problems with down-conversion at frequencies close to the resonance condition may also arise because there will be a strong frequency dependence of the conversion efficiency. We have therefore studied the frequency dependence of the down-converted signal amplitude (or conversion efficiency), keeping all other parameters fixed. To quantify the conversion efficiency, we suppose that the power necessary for controlling the absorber is negligible, and the RF power applied to the system is due to the variation of the threshold current by absorber modulation. We then estimate the efficiency using (5) and supposing  $P_s = \hbar\omega \cdot \Delta I_{th} \cdot V$ . The result is shown in Fig. 5. It is clear that this curve is similar to the well-known current modulation characteristics [17] of semiconductor lasers. Such a result is, indeed, implied by (3) with its resonant denominator, although strictly speaking, because (3) is obtained using lumped parameters, it is not applicable when the signal and LO frequencies are close to that of the round trip (also, the difference-frequency modulation near resonance is strong so the small-signal theory cannot be expected to hold exactly). Besides exhibiting a sharp resonance in the vicinity of  $f_{res}$ , the curve in Fig. 5 also contains a flat section at frequencies  $f < f_{res}$ . The former frequency regime should therefore be advantageous for down-conversion of narrowband modulated signals, and the latter for broadband modulated signals.

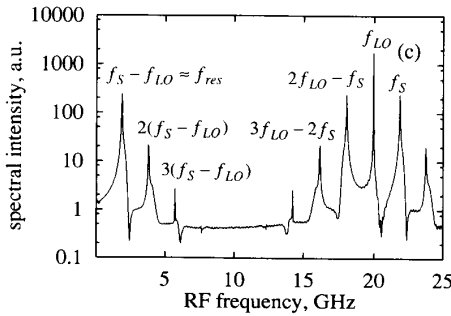
3) *Up-Conversion*: In all the cases so far considered, sum frequencies are always generated along with difference frequencies, i.e., up-conversion always accompanies down-conversion. As can be seen in Fig. 6(a), which simply shows a higher frequency section of the spectrum of Fig. 4(c), the intensity of the up-converted signal is approximately the same as that of the down-converted signal. The high absolute value of the up-converted intensity is due to the system being close to the resonance condition. Fig. 6(b) illustrates a more isolated case of up-conversion, in which  $f_{res} < f_S < f_{LO} - f_{res}$ . One notices that even in this case, clearly the least advantageous being far from of all possible resonant conditions, the intensity



(a)



(b)



(c)

Fig. 4. (a) Part of the RF spectrum of a free-running, mode-locked, extended-cavity laser emission; parameters as in Table I, pumping current  $J/J_{th} = 4.5$ . (b) and (c) The low-frequency part of the emission spectrum from the same laser, under direct modulation of the unsaturated absorption of an amplitude  $\Delta a/g_{th} = 0.02$ . (b) Modulation frequency  $f_S = 20.5$  GHz. (c)  $f_S = 22.2$  GHz.

of the up-converted line still reaches a significant value of about  $-40$  dB with respect to the main  $f_{LO}$  line. One can therefore anticipate that this principle of up-conversion, when combined with the latest achievements in ultrahigh-frequency modelocking [5], [6], may be useful in generating millimeter-wave amplitude modulated optical signals. Besides the up-converted peak at  $33$  GHz  $= f_{LO} + f_S$ , Fig. 6 also contains a peak at  $27$  GHz  $= 2f_{LO} - f_S$ . In order to observe up-conversion more clearly, it would be desirable if the initial mode-locking signal (the local oscillator) were to contain only one frequency component, i.e., to be a sinusoidal signal. This is often the case in high-frequency mode-locking schemes [5], [6], when only two or three longitudinal cavity modes are observed in the mode-locked spectra. The analysis of this

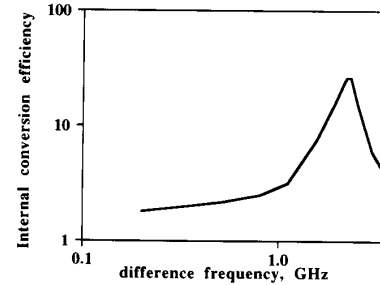
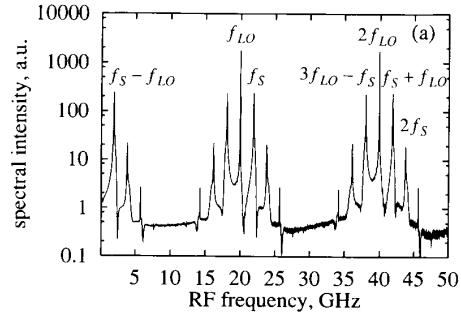
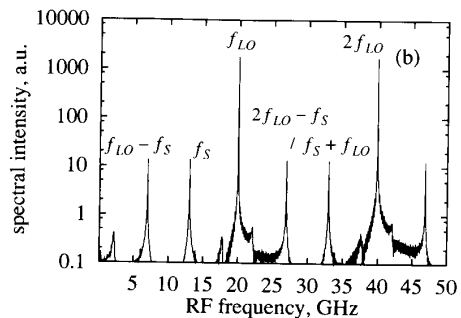


Fig. 5. Difference frequency dependency of the intensity of the fundamental down-converted line in the spectra of the same laser shown in Fig. 4.



(a)



(b)

Fig. 6. Part of emission spectra from the same laser as in Fig. 4 and 5, modulated with the same amplitude  $\Delta a/g_{th} = 0.02$ , at frequencies (a)  $f_S = 22.2$  GHz and (b)  $f_S = 13.0$  GHz.

situation is, however, beyond the scope of the present paper, a detailed investigation into the high-frequency case being reserved for future studies.

### III. EXPERIMENTAL

As has been shown above, the fundamental physics of frequency mixing is essentially the same regardless of the regime ( $Q$ -switching or mode-locking) and the range of frequencies involved. Therefore, in order to demonstrate the feasibility of optoelectronic up- and down-conversion, experiments performed so far have been carried out using signals in the range 1–2 GHz from a passively  $Q$ -switched QW laser diode.

#### A. Device Fabrication

The passively  $Q$ -switched laser used in the experiment was based on a ridge waveguide structure with a ridge width of

3.5  $\mu\text{m}$ . The active region consisted of two 6-nm-thick strained InGaAs wells separated by 2-nm-thick GaAs barriers giving an operating wavelength of 960 nm. The total cavity length of the device was 400  $\mu\text{m}$  (Fig. 1(b)). The p-type contact was separated into two sections, one of which formed a contact to the gain section, and the other to an electroabsorption loss modulator (the saturable absorber). The two contacts were electrically isolated by selectively etching a 20- $\mu\text{m}$  gap in the GaAs<sup>p+</sup> contact layer to give an isolation resistance between the two regions of 2 k $\Omega$ . The length of the saturable absorber was 30  $\mu\text{m}$  and the threshold current of the device with both sections in forward bias was 9 mA.

### B. Measurement System

The self-pulsation frequency of the laser was measured by focusing the cw train of pulses onto a fast InGaAs photodetector with a bandwidth of 20 GHz. The electrical signal from the photodiode was then connected to a RF spectrum analyzer with a resolution of 100 kHz.

### C. Experimental Results

When driven with a cw current of 80 mA through the gain section and 1.6 V reverse bias across the saturable absorber, the two-section laser demonstrated *Q*-switching operation as shown in Fig. 7(a). The *Q*-switched pulses result in a number of spectral peaks in the frequency domain. The (fundamental) *Q*-switching frequency of around 1.5 GHz and its second harmonic at 3.0 GHz are shown in Fig. 7(a). Further harmonics were observed at higher frequencies. Note that the amplitude of the second harmonic is approximately 10 dB below that of the fundamental *Q*-switching line, which shows that the pulses generated are not far from sinusoidal, the measurement system being unlikely to introduce distortions at frequencies measured.

The addition of an RF signal to the gain section of the laser alters radically the RF spectrum of the optical output. Fig. 7(b) shows the result of applying a -14.3 dBm, 1.47 GHz RF signal to the gain section. The first point to note is that for -14.3 dBm applied RF power, the *Q*-switching (local oscillator) frequency is not pulled toward the RF signal frequency. In the course of these experiments, the *Q*-switching frequency varied through the range 1.45 to 1.55 GHz with no applied RF signal, which we attribute to temperature drift, hence the change in *Q*-switching frequency between Fig. 7(a) and (b).

The most pronounced influence of the application of the RF signal is the additional spectral peaks at 1.64 GHz and 3.02 GHz. The first of these peaks can be attributed to mixing of the applied RF signal with the 2nd harmonic of the *Q*-switching frequency. The peak at 1.64 GHz is the *down-converted* signal resulting from the mixing process (3.11–1.47 GHz). The second peak can be ascribed to mixing of the applied RF signal with the fundamental *Q*-switching frequency. The peak at 3.02 GHz is the *up-converted* signal resulting from the mixing process (1.55 GHz + 1.47 GHz).

This demonstrates that both up- and down-conversion processes occur, and that mixing occurs not only between the

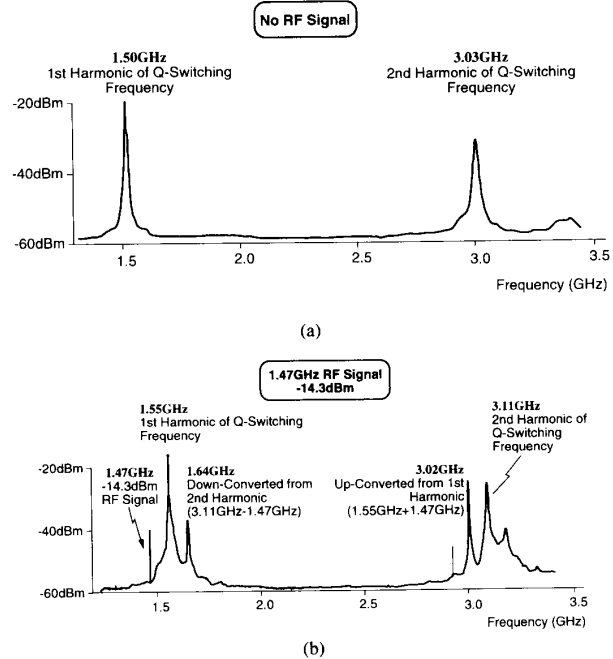


Fig. 7. Frequency spectra of two-section laser with (a) no RF signal applied to gain section and (b) with 1.47-GHz applied RF signal.

signal and the fundamental frequency of the laser, but also with the harmonics of the laser LO frequency.

Further evidence that the spectral peaks arising from the addition of an RF signal are due to up- and down-conversion can be obtained by changing the frequency of the applied RF signal. In Fig. 8(a), the signal frequency is again 1.47 GHz, while in Fig. 10(b), the signal frequency is reduced to 1.40 GHz. In both cases, the applied signal is at a power of -14.3 dBm, and the dc bias conditions of the two-section laser are 80 mA drive current to the active section and 1.6 V reverse bias across the saturable absorber. Consider first Peak A, which occurs at 1.64 GHz, in the spectrum of Fig. 8(a). We have postulated that this peak is the down-converted signal resulting from mixing of the applied RF signal and the 2nd harmonic of the *Q*-switched frequency. Reducing the frequency of the applied RF signal from 1.47 GHz to 1.40 GHz causes Peak A to increase from 1.64 GHz to 1.71 GHz, as expected if this spectral peak were the result of a down-conversion process. Similarly, reducing the signal frequency causes Peak B (3.02 GHz in Fig. 8(a)) to decrease to 2.96 GHz (Fig. 8(b)), as would be expected if this spectral peak were the up-converted signal resulting from mixing of the signal frequency and the *Q*-switching LO frequency.

Yet more evidence that mixing is occurring can be found by studying the dependence of the measured RF spectra of the optical output of the laser on the power of the applied signal. Fig. 9 shows these spectra in the frequency range 1.2 GHz to 3.5 GHz for increasing applied signal powers. Note that in the range -25 dBm to -10 dBm, the fundamental *Q*-switched LO frequency is essentially independent of the signal power. For -25 dBm applied signal power, there is

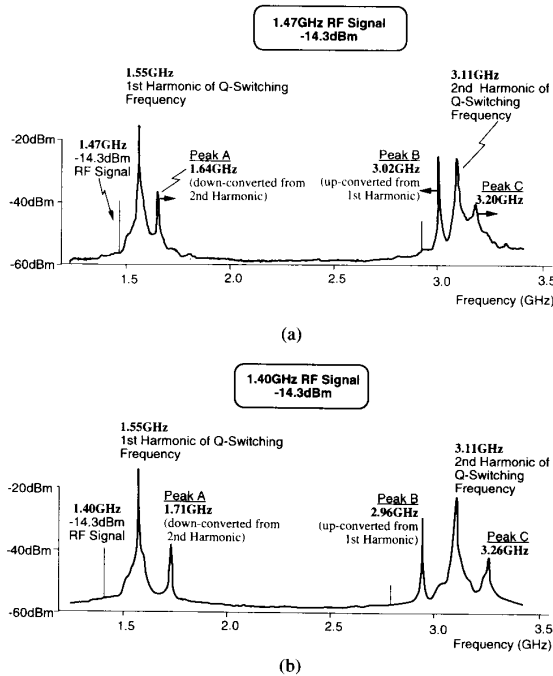


Fig. 8. Frequency spectra of two-section laser with RF signals of (a) 1.47 GHz and (b) 1.40 GHz applied to gain section.

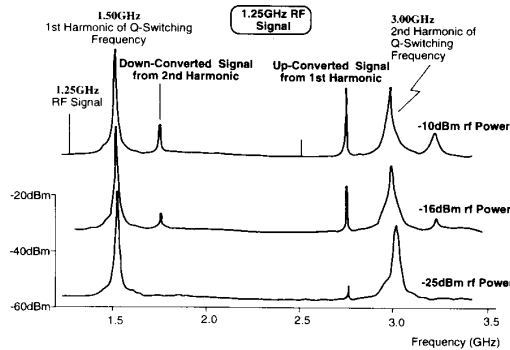


Fig. 9. Frequency spectra of two-section laser with 1.25 GHz RF signals of (a) power  $-25$  dBm, (b)  $-16$  dBm, and (c)  $-10$  dBm applied to gain section.

some evidence of the up-conversion occurring from mixing between the signal frequency and the  $Q$ -switching LO. As the RF power is increased to  $-16$  dBm, the down-converted signal from mixing between the signal and the 2nd harmonic of the  $Q$ -switching LO becomes apparent. At  $-10$  dBm, the up-converted and 2nd harmonic signals have similar magnitude. For applied powers of greater than  $-5$  dBm, the  $Q$ -switching frequency starts to be pulled toward that of the applied RF signal.

Fig. 10(a) shows the output RF spectrum around the fundamental  $Q$ -switching frequency in the frequency range 0.5 GHz to 2.5 GHz for no applied RF signal. Again, the dc conditions are 80 mA cw drive current through the gain section, and 1.5 V reverse bias across the saturable absorber. Fig. 10(b)

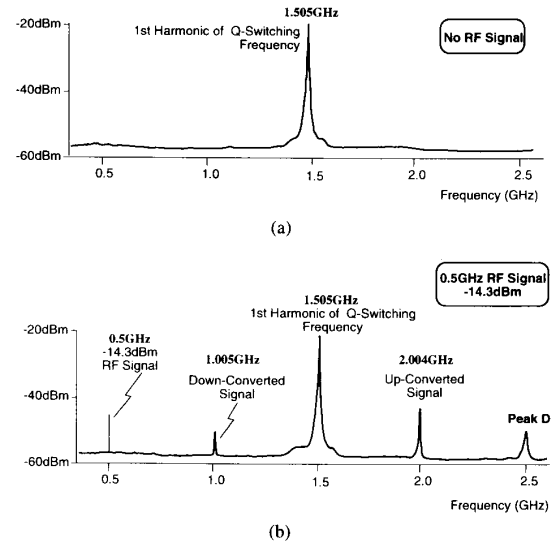


Fig. 10. Frequency spectra of two-section laser with (a) no RF signal applied to gain section and (b) with 0.5-GHz applied RF signal.

shows the same frequency range with a  $-14.3$  dBm, 0.5 GHz signal applied to the gain region of the laser. Both the up- and down-converted signals resulting from mixing of the RF signal and the  $Q$ -switching are apparent at 1.005 GHz and 2.004 GHz, respectively.

#### D. Determination of Conversion Efficiencies

As discussed in Section II-B, when acting as a mixer, the conversion efficiency of the laser can be defined as  $\eta = (P_2/P_s)$  where  $P_2$  is the optical power at the sum and difference frequencies  $f_2 = f_{LO} \pm f_s$ , and  $P_s$  is the input microwave signal power.

To determine the optical power at the sum and difference frequencies, the total laser output power, corresponding to the integrated intensity of all peaks in the frequency spectrum, was first measured. The integrated intensity of individual up or down converted peaks was then evaluated and compared with the total integrated intensity from all spectral peaks, giving the optical power in the sum and difference signals. The magnitude of the microwave signal into the laser was determined by measuring the microwave reflection coefficient of the laser while accounting for losses in the system. This also permitted the magnitude of the RF input current to be determined.

These measurements were performed on a two-section laser with a self-pulsation frequency of 1.5 GHz when driven with a current of 80 mA, and a 0.9-GHz RF signal applied to the gain section. Fig. 11 shows the experimental conversion efficiency of both the up- and down-conversion processes due to mixing of the first harmonic of the  $Q$ -switching frequency with the applied RF signal, as a function of input RF current (normalized to the threshold current of the device when fully forward biased (20 mA in this case)). Theoretical values of conversion efficiency, derived in Section II-B, are also plotted in Fig. 11. In both experimental and theoretical cases, up-conversion is observed to be more efficient than the down-



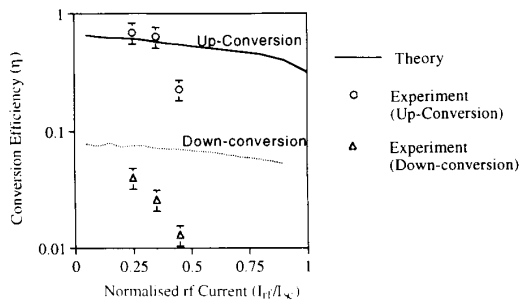


Fig. 11. Comparison of experimental and theoretical up- and down-conversion efficiencies for mixing of first harmonic of  $Q$ -switching frequency and input RF signal.

conversion process by approximately an order of magnitude. We are currently performing further work to understand the basis of this phenomena, which we shall report upon at a later date.

#### IV. CONCLUSIONS

Optoelectronic mixing of very high-frequency amplitude modulated signals in semiconductor lasers has been studied theoretically. Three possible constructions have been proposed for a laser-mixer capable of working simultaneously as a local oscillator and a mixing element. These constructions include four-terminal lasers with dual (pumping and confinement) modulation, and both externally modulated passively  $Q$ -switched and externally modulated passively mode-locked lasers. The laser mixers provide their output in the form of an optical signal modulated at sum and difference of the local oscillator and signal frequencies. It has been shown that the fundamental physics of frequency mixing is based on parametric effects and is essentially the same for all the three cases studied. For the case of dual modulation, analytical estimates for the conversion efficiency have been obtained in the small-signal approximation. For the case of a passively mode-locked laser, the frequency dependence of the down conversion efficiency has been studied numerically and shown to be of a resonant type similar to the modulation response of a laser diode. Additional spectral lines have been shown to arise due to mixing with higher harmonics of the local oscillator, and the use of mode-locked lasers with spectral properties engineered to provide nearly sinusoidal mode-locked pulses suggested as a way of avoiding the generation of these lines. An experimental confirmation of the feasibility of the laser-mixer was obtained using a  $Q$ -switched laser diode. Future work will concentrate on experimental and theoretical studies of frequency-mixing at submillimeter frequencies using short-cavity mode-locked lasers; other matters reserved for future studies are to line-narrow the microwave spectrum of the LO for practical applications and to measure the absolute conversion efficiency and phase noise.

#### REFERENCES

[1] A. J. Seeds, "Microwave optoelectronics," *Opt. Quantum Electron.*, vol. 25, pp. 219–229, 1993.

- [2] V. B. Gorfinkel, G. Kompa, M. Novotny, S. A. Gurevich, G. E. Shtengel, and I. E. Chebunina, "High-frequency modulation of a QW diode laser by dual modal gain and pumping current control," in *Proc. Int. Electron. Device Meeting, IEDM'93*, 1993, p. 933.
- [3] V. B. Gorfinkel, S. A. Gurevich, I. E. Chebunina, M. S. Shatalov, and G. E. Shtengel, "High-frequency operation of heterostructure diode laser modulated by dual optical confinement factor and pumping density control," *IEEE J. Quantum Electron.*, submitted.
- [4] E. L. Portnoi and A. V. Chelnokov, "Passive mode-locking in a short cavity diode laser," in *Dig. 12th IEEE Int. Semiconductor Laser Conf.*, Davos, Switzerland, 1990, p. 140–141.
- [5] J. M. Martins-Filho, E. A. Avrutin, C. N. Ironside, and J. S. Roberts, "Mode-locked quantum-well lasers: Experiment and theory," this issue, pp. 539–551.
- [6] S. Arakura, S. Oshiba, Y. Matsui, T. Kunii, and Y. Ogawa, "Terahertz-rate optical pulse generation from a passively mode locked semiconductor laser diode," *Optics Lett.*, vol. 19, pp. 834–836, 1994.
- [7] J. H. Zarrabi, E. L. Portnoi, and A. V. Chelnokov, "Passive mode-locking of a multistriple single quantum well GaAs laser diode with an intra-cavity saturable absorber," *Appl. Phys. Lett.*, vol. 59, pp. 1526–1528, 1991.
- [8] E. A. Avrutin, V. B. Gorfinkel, S. Luryi, and K. A. Shore, "Control of surface-emitting laser diodes by modulating the distributed Bragg mirror reflectivity: Small-signal analysis," *Appl. Phys. Lett.*, vol. 63, pp. 2460–2462, 1993.
- [9] E. A. Avrutin, "Spontaneous emission and noise in self-pulsing semiconductor lasers," in *IEE Proc. Pt. J.*, vol. 140, pp. 16–20, 1993.
- [10] K. A. Shore and M. W. McCall, "Nonlinear and quantum optics in semiconductor lasers," *Prog. Quant. Electron.*, vol. 14, pp. 63–127, 1991.
- [11] U. Feiste, M. Moerle, B. Sartorius, J. Hoerer, and R. Loeffler, "12 GHz to 64 GHz continuous frequency tuning in selfpulsating 1.55  $\mu\text{m}$  quantum well DFB lasers," in *Dig. 14th IEEE Semiconductor Laser Conf.*, 1994, paper Th2.3.
- [12] A. G. Weber, M. Schell, G. Fischbeck, and D. Bimberg, "Generation of single femtosecond pulses by hybrid mode locking of a semiconductor laser," *IEEE J. Quantum Electron.*, vol. 28, pp. 2220–2229, 1992.
- [13] M. Schell, A. G. Weber, E. Schoell, and D. Bimberg, "Fundamental limits of sub-ps pulse generation by active mode locking of semiconductor lasers: The spectral gain width and the facet reflectivities," *IEEE J. Quantum Electron.*, vol. 27, pp. 1661–1668, 1991.
- [14] J. H. Marsh, "Quantum-well intermixing," *Semicond. Sci. Technol.*, vol. 8, pp. 1136–1155, 1993.
- [15] E. A. Avrutin, V. B. Khalfin, J. M. Arnold, and J. H. Marsh, "Time- and frequency domain theory of externally synchronised operation of a passively mode locked laser diode," in *Tech. Dig. Conf. Lasers Electro-Optics*, Europe, 1993, paper CTuE6, p. 76.
- [16] V. B. Khalfin, J. M. Arnold, and J. H. Marsh, "Synchronization of a mode-locked laser with an external pulse stream," this issue, pp. 523–527.
- [17] R. G. Hunsperger, *Integrated Optics: Theory and Technology*. New York: Springer, 1991, p. 241.

**Efim L. Portnoi** (M'94) was born in Kursk, Russia, in July 1938. He graduated in 1962, with honors, from Leningrad Polytechnic Institute (presently St. Petersburg Technical University) and was awarded a Ph.D. in Semiconductor Physics (1970) from the A. F. Ioffe Physico-Technical Institute (PTI).

From 1964 to the present, he has been a member of the Research Staff of the A. F. Ioffe PTI, Russian Academy of Sciences, St. Petersburg. He is currently a Distinguished Member of the Research Staff, Head of the Integrated Optics Laboratories, A. F. Ioffe PTI. Since 1983, he has been a professor at St. Petersburg Technical University, lecturing in Semiconductor Lasers and Integrated Optics and, since 1993, visiting professor at the Department of Electronics and Electrical Engineering the University of Glasgow. His major professional achievements include: 1) Creation of the world's first ideal heterojunctions and low-threshold double heterostructure lasers based on AlAs–GaAs solid solutions (1968, together with Zh. I. Alferov *et al.*); and 2) elaboration of the physical and technological principles of integrated optics based on heterostructures and the creation of new integrated optical devices, including distributed-feedback lasers and picosecond optical pulse generators.

Prof. Portnoi is a member of the editorial boards of two scientific journals, *Pisma v Zh. Tekh. Fiz.* (English translation: *Sov. Tech. Phys. Lett.*) and *Zh. Tekh. Fiz.* (English translation: *Sov. Phys. Tech.*). He has published more than 150 journal papers, and is the holder of 36 Soviet patents.

**Vera B. Gorfinkel** received the Ph.D. degree in semiconductor physics, in 1980, from the Ioffe Physico-Technical Institute, St. Petersburg, Russia.

She worked at the Institute for Radioelectronics, USSR Academy of Sciences until 1991. Since 1991, she has been with the University of Kassel, Germany. Her main research interests are in the physics of exploratory high-frequency semiconductor optoelectronic devices.



**Eugene A. Avrutin** was born in Leningrad, USSR (presently St. Petersburg, Russia), in 1963. He received the M.Sc. degree (with honors) from Leningrad Polytechnical Institute (presently St. Petersburg Technical University), in 1986.

Since then, he was with A. F. Ioffe Physico-Technical Institute, St. Petersburg, working on theory and numerical modelling of semiconductor lasers and integrated waveguide devices, and in 1993 completed his Ph.D. in this field. In 1991, he was a visiting scientist at the University of Kassel, Germany, and he spent the year of 1992 at the School of Electronics and Electrical Engineering of the University of Bath, UK, under Royal Society Academic Exchange Fellowship. Since 1993, Dr. Avrutin is with the Department of Electronics and Electrical Engineering at the University of Glasgow. His current research interests include theory and numerical modelling of semiconductor lasers with the emphasis on fast dynamics and system applications.



**Iain G. Thayne** was born in Glasgow, in June 1965. He gained a first class honors degree in physics and electronic engineering at the University of Glasgow, in 1986. From there, he moved to Philips Research Laboratories, Redhill, Surrey, where he worked on the fabrication and characterization of high electron mobility transistors (HEMT's).

In 1988, he returned to Glasgow University as a research assistant in the Department of Electronics and Electrical Engineering, and in 1992, completed the Ph.D. degree for work on the fabrication and

high-frequency characterization of short-gate-length heterojunction field effect transistors (HFET's), including the fabrication of state-of-the-art sub-100-nm gate-length HFET's with  $f_T$  of 275 GHz. In 1992 he also worked as a consultant to the Microwave Systems Group at Norwegian Telecom Research in Kjeller, Norway. His current research interests include the millimeter-wave performance of short-gate-length transistors, the design and fabrication of microwave signal processing circuits, low-noise cryogenic electronics, low-dimensional transport devices, and microwave optoelectronic devices and circuits.

Dr. Thayne currently holds an EPSRC Postdoctoral Research Fellowship to design and fabricate low-noise, cryogenic detection electronics for nanostructures.



**David A. Barrow** was born in Guildford, England, in 1967. He received the B.Sc. degree in engineering with honors from the University of Dundee, Scotland, in 1991. His research interests are in the area of optoelectronic device design and fabrication. He is currently writing a Ph.D. thesis at the University of Glasgow, investigating ultrafast optical pulse generation and detection using semiconductor devices. His Ph.D. work is supported by the Science and Engineering Council and by BNR Europe.



**John H. Marsh** (M'91-SM'91), was born in Edinburgh, Scotland, in 1956, but was brought up and educated in Glasgow. He received the B.A. degree in engineering and electrical sciences from the University of Cambridge, in 1977, the M.Eng. degree in solid-state electronics from the University of Liverpool, in 1978, and the Ph.D. degree from Sheffield University, in 1982, with research in the LPE growth and electrical transport properties of InGaAsP alloys.

He has been a reader in the Department of Electronics and Electrical Engineering at Glasgow University, since 1994, having previously been appointed lecturer, in 1986, and senior lecturer, in 1990. His present research interests are particularly concerned with linear and nonlinear integrated optoelectronic devices in III-V semiconductors. He has developed new integration technologies for photonic integrated circuits based on quantum-well devices and quantum-well intermixing.

John Marsh is a member of the Institution of Electrical Engineers (IEE) and of the British Association for Crystal Growth. He has served as a member of the IEEE Professional Group concerned with Optical Devices and Systems (1988-1994) and a corresponding editor of the *IEEE Electronics and Communication Journal*. He directed the NATO Advanced Study Institute on Waveguide Optoelectronics held in Glasgow, in 1990, and is co-editor of the book with the same name. He is author or coauthor of more than 140 journal and conference papers.

**Serge Luryi** (M'81-SM'85-F'90), received the Ph.D. degree in physics from the University of Toronto, in 1978.

Between 1980 and 1994, he was a Member of Technical Staff at AT&T Bell Laboratories in Murray Hill. During this period he served as a Group Supervisor in several device research departments, dealing with VLSI, Quantum Phenomena and Optoelectronics. In 1990, Bell Laboratories recognized him with the Distinguished Member of Technical Staff award. In 1994, Dr. Luryi joined the faculty of the State University of New York at Stony Brook, where is currently a Leading Professor and Chairman of the Department of Electrical Engineering.

Dr. Luryi served on the Editorial Board of IEEE Transactions on Electron Devices, first as an associate editor and then as the Editor, from 1986-1990. In 1989, Dr. Luryi was elected Fellow of the IEEE "for contributions in the field of heterojunction devices," and in 1993, Fellow of the American Physical Society "for theory of electron transport in low-dimensional systems and invention of novel electron devices." He has published over 130 papers and filed 26 US patents in the areas of high-speed electronic and photonic devices, material science, and advanced packaging.